

Fast Spectral-Based Separation of Multispectral Images

Philipp Urban, Mitchell R. Rosen, Roy S. Berns;
Munsell Color Science Laboratory, Chester F. Carlson Center for Imaging Science,
Rochester Institute of Technology, 54 Lomb Memorial Drive, Rochester, New York 14623

Abstract

In this paper we present an algorithmic framework for spectral separation of multispectral images. The proposed iterative method inverts the widely used cellular Yule-Nielsen spectral Neugebauer printer model so quickly that model inversion can be considered for pixel-by-pixel application. Simplification and precalculation make improvements and small modifications of the algorithm significantly reduce the computational effort. Using today's available standard hardware allows the separation of high resolution multispectral images in reasonable time.

Introduction

Spectral separation of multispectral images enables a hardcopy reproduction whose color accuracy is observer and illuminant independent. This is an advantage compared to traditional printing methods (e.g. ICC [1]) that adjust the reproduction to a specific illuminant and observer. Traditional methods are therefore afflicted with systematic problems such as observer and illuminant metamerism if the viewing conditions change.

Unfortunately, typical printing systems are physically limited in reflectance spectra they can produce. Spectral gamut mapping is thus necessary [2]. Therefore an errorless spectral reproduction is, in general, not realizable. Nevertheless, the metamerism can be minimized [3], the color constancy index can be maximized [4] or other characteristics for spanning multiple light sources can be improved.

After compressing the image to the spectral gamut of the rendering device, suitable printer control values have to be found to reproduce these spectra. This can be done by inverting a spectral printer model.

A spectral printer model is a prediction function from control value space into spectral space. Various models have been proposed in the past [5]. Because of its simplicity and accuracy the Yule-Nielsen spectral Neugebauer (YNSN) model [6, 7, 8, 9, 10, 11] and its cellular extension [12] the cellular Yule-Nielsen spectral Neugebauer (CYNSN) model are widely used in practice.

Since the YNSN model is analytically not invertible, different iterative methods have been proposed that use standard numerical optimization techniques [13, 14, 15]. To invert the CYNSN model gradient-based methods should not be used without modification since the model is not differentiable on the cell boundaries.

In this paper we present a fast and simple iterative algo-

rithm to invert the CYNSN model. This method can be used to separate multispectral images on a pixel by pixel basis. The proposed algorithm is based on recent work to invert the YNSN model [16], a modification to accelerate the inversion [17] and a method that considers the transition between cells of the CYNSN model [18]. In this paper we combine these approaches and present the whole system that allow a simple and fast inversion of the CYNSN model. The article should enable the reader to reimplement the algorithm.

The Cellular Yule-Nielsen modified Neugebauer Model (CYNSN)

The accuracy of the CYNSN model improves in general the accuracy of the plain YNSN model since the physical printer transfer function is sampled on more than the 2^m Neugebauer primaries for a m colorant printer. The drawback is the need of more measurements. Therefore it is necessary to find a good compromise between measurement effort and spectral accuracy. In our work we consider only regular subdivisions. But also other subdivisions are possible [19]. Figure 1 shows a subdivision of the CMY space with 8 cells. To fit the model to the printer all reflectance spectra corresponding to the cell vertices have to be printed and measured. For a regular grid with k grid points in each dimension k^m patches have to be measured. The CYNSN model has than $(k-1)^m$ cells and each cell has 2^m vertices that we denote in control value space by

$$v_{I_0}, \dots, v_{I_{2^m-1}} \in [0, 1]^m \quad (1)$$

and the corresponding spectra in reflectance space

$$R_{I_0}, \dots, R_{I_{2^m-1}} \in [0, 1]^N \quad (2)$$

where $I \in \{0, \dots, k-1\}^m$ is a multi-index describing the cell and $j = 0, \dots, 2^m - 1$ numbers the vertices within the cell. For a CMY printer this is

$$\begin{aligned} I_0 &= I + (0, 0, 0) & I_1 &= I + (0, 0, 1) \\ I_2 &= I + (0, 1, 0) & I_3 &= I + (0, 1, 1) \\ I_4 &= I + (1, 0, 0) & I_5 &= I + (1, 0, 1) \\ I_6 &= I + (1, 1, 0) & I_7 &= I + (1, 1, 1). \end{aligned}$$

In Figure 1 the cell $I = (0, 1, 1)$ is emphasized. The CYNSN model for a CMY printer has the following form in each cell:

$$R(C, M, Y) = \left[\sum_{i=0}^7 a_{I_i}(C, M, Y) R_{I_i}^{1/n} \right]^n \quad (3)$$

where I is the multi-index of the cell that contains the C, M, Y values, n is the so called Yule-Nielsen factor that empirically models

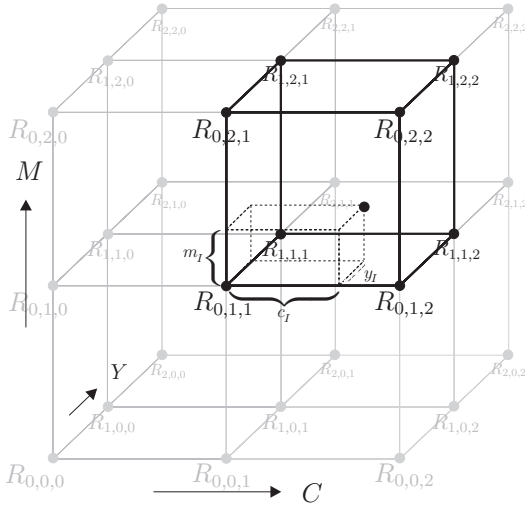


Figure 1. Partition of the colorant space into smaller cells for a CMY printer

the optical dot gain and $a_i(C, M, Y)$ are the Demichel equations:

$$\begin{aligned}
 a_0(C, M, Y) &= (1 - c_I)(1 - m_I)(1 - y_I) \\
 a_1(C, M, Y) &= c_I(1 - m_I)(1 - y_I) \\
 a_2(C, M, Y) &= (1 - c_I)m_I(1 - y_I) \\
 a_3(C, M, Y) &= c_I m_I(1 - y_I) \\
 a_4(C, M, Y) &= (1 - c_I)(1 - m_I)y_I \\
 a_5(C, M, Y) &= c_I(1 - m_I)y_I \\
 a_6(C, M, Y) &= (1 - c_I)m_I y_I \\
 a_7(C, M, Y) &= c_I m_I y_I
 \end{aligned}$$

Here the c_I , m_I and y_I are the effective area coverages normalized to the cell primaries, i.e. for primaries $v_i = [v_i^C, v_i^M, v_i^Y]^T$, $i = 0, \dots, 7$:

$$\begin{aligned}
 c_I &= (v_7^C - C)/(v_7^C - v_0^C) \\
 m_I &= (v_7^M - M)/(v_7^M - v_0^M) \\
 y_I &= (v_7^Y - Y)/(v_7^Y - v_0^Y)
 \end{aligned}$$

To use the CYNSN model the theoretical control values have to be transformed into effective area coverages using typically one dimensional lookup tables (see e.g. [5]).

The model can be easily expanded on printers with more than three colorants.

Inversion of the CYNSN model

The proposed algorithm is composed of three parts:

1. A method for inverting the plain YNSN model.
2. A method that perform the transitions of the iteration from one cell to a neighboring cell
3. A small modification to reduce the number of multiplications in each iteration step and therefore to accelerate the inversion significantly.

Inversion of the plain YNSN model

Urban et al. [16] proposed a simple method to invert the plain YNSN model called the Linear Regression Iteration (LRI) method. The LRI method utilizes a special property of the YNSN model, i.e. to be multi-linear in $1/n$ -space. The following optimization problem for the inversion is considered by the LRI method

$$\|R(\psi)^{1/n} - r^{1/n}\|_2 = \min \quad (4)$$

subject to

$$\psi \in [0, 1]^m \quad (5)$$

where $\psi = (\psi_1, \dots, \psi_m)$ is the vector of effective area coverages, $R(\psi)$ is the YNSN model (this equals the model in eq. 3 with only one cell) and r is the reflectance spectrum to be reproduced. Here we use discrete reflectances resulting from an sampling at N equidistant wavelength position, i.e. r , $R(\psi)$ are N dimensional vectors. Typically a sampling in 10 nm intervals between 400 nm - 700 nm is used, which results in $N = 31$.

It should be noticed that for reflectances within the spectral gamut of the printer the objective function vanishes. For out-of-gamut reflectances an implicit gamut mapping is performed that minimizes the RMS difference in $1/n$ -space.

Since the YNSN model is multi-linear in $1/n$ -space it can

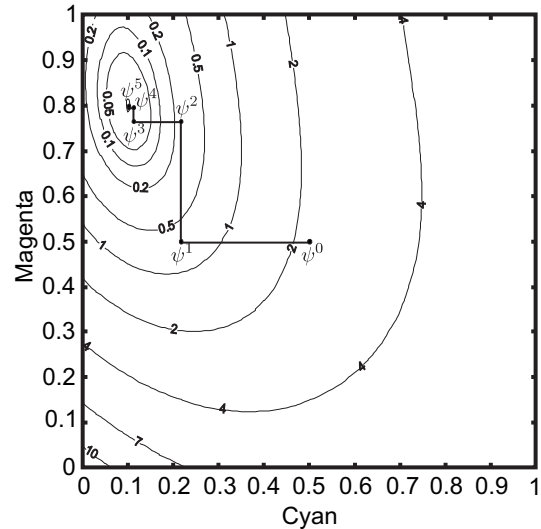


Figure 2. Iteration sequence of the LRI method for a printer using only cyan and magenta.

be decomposed as follows

$$R(\psi)^{1/n} = \vec{A}_i(\psi) \cdot \psi_i + \vec{B}_i(\psi) \quad (6)$$

where $\vec{A}_i(\psi)$ and $\vec{B}_i(\psi)$ are N -dimensional vectors independent of ψ_i .

The colorant ψ_i that minimizes the objective function by holding the other colorants fixed can be simply calculated using linear regression, i.e.

$$\psi_i^{OPT} = \frac{\vec{A}_i(\psi)^T (\vec{B}_i(\psi) - r^{1/n})}{\vec{A}_i(\psi)^T \vec{A}_i(\psi)} \quad (7)$$

Iterating this equation by successively recalculating the colorants and considering the constraint leads to the LRI algorithm with starting point $\psi^0 = (\psi_1^0, \dots, \psi_m^0)$

1. REPEAT {
2. FOR ($i = 1; i \leq m; i = i + 1$) {
3. $\psi_i = D \left[\frac{\bar{A}_i(\psi)^T (\bar{B}_i(\psi) - r^{1/n})}{\bar{A}_i(\psi)^T \bar{A}_i(\psi)} \right];$
4. }
5. } UNTIL TERMINATION;

where the constraints are considered by the clipping function D

$$D[x] = \begin{cases} 0, & x < 0 \\ 1, & x > 1 \\ x, & \text{otherwise} \end{cases} \quad (8)$$

Possible termination criteria are described in [16] where also a complexity estimation is presented concerning multiplication operation.

The advantage of the LRI method compared to Newton-based methods is its simplicity and the small number of multiplication operation in each iteration step. Neither gradients or Hesse-matrices need to be calculated, nor linear equation systems have to be solved. The whole calculation in each iteration step consists mainly in two simple matrix-vector multiplication that are sufficient to calculate $\bar{A}_i(\psi)$ and $\bar{B}_i(\psi)$:

$$\bar{A}_i(\psi) = A_i \cdot \bar{v}_i(\psi) \quad (9)$$

$$\bar{B}_i(\psi) = B_i \cdot \bar{v}_i(\psi) \quad (10)$$

where A_i and B_i are $N \times 2^m$ dimensional matrices that are independent on colorants and need to be calculated only once for each YNSN model by simply expanding and rearranging the model. The vector $\bar{v}_i(\psi)$ has to be calculated for each iteration step and includes the monomials of the colorants except ψ_i , i.e.

$$\bar{v}_i(\psi) = w_{m-1}(\psi) \quad (11)$$

where

$$\begin{aligned} w_1(\psi) &= \begin{bmatrix} 1 \\ \psi_{i_1} \end{bmatrix}, \\ w_2(\psi) &= \begin{bmatrix} w_1(\psi) \\ \psi_{i_2} \cdot w_1(\psi) \end{bmatrix}, \\ &\vdots \\ w_{m-1}(\psi) &= \begin{bmatrix} w_{m-2}(\psi) \\ \psi_{i_{m-1}} \cdot w_{m-2}(\psi) \end{bmatrix} \end{aligned}$$

with $i_j < i_{j+1}$ and $i_j \neq i$.

The order of convergence of the LRI method is linear, where Newton-like methods can achieve a quadratic convergence order near the solution. Therefore, the LRI method needs in general more, but computationally less expensive, iteration steps.

Transition of the LRI-Iteration from Cell to Cell of a CYNSN Model

Urban et al. [18] presented a technique to expand the LRI method to the CYNSN model, the so called cellular LRI (CLRI)

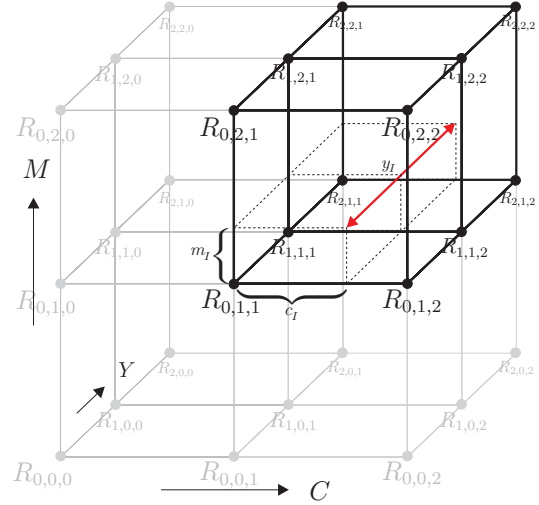


Figure 3. Holding C and M fixed, the search domain (red arrow) for the optimal Y value covers two cells (black emphasized).

method. Since in each iteration step of the LRI method only one colorant is changed by holding the other colorants fixed, a similar approach can be used by considering more cells. Holding $m - 1$ colorants fixed the domain of the remaining colorant spans only $k - 1$ cells. Therefore maximal $k - 1$ linear regressions are necessary to find the optimal colorant that minimizes the objective function holding the other colorants fixed.

The pre-calculated matrices introduced in eq. (9) and (10) can be calculated for each cell of the CYNSN model in advance. To allow a fast access to the matrices they can be arranged to a special matrix scheme. For each cell I the following $N \times (m \cdot 2^m)$ matrices can be formed:

$$AB^I = [A_1^I, B_1^I, \dots, A_m^I, B_m^I] \quad (12)$$

By ordering all of these matrices according their multi-indices the following matrix scheme can be constructed:

$$AB = \begin{bmatrix} AB^{(0,\dots,0)} \\ AB^{(0,\dots,1)} \\ \vdots \\ AB^{(0,\dots,k-2)} \\ AB^{(0,\dots,1,0)} \\ \vdots \\ AB^{(k-2,\dots,k-2)} \end{bmatrix} \quad (13)$$

The final matrix has the dimension $N \cdot (k - 1)^m \times (m \cdot 2^m)$.

Holding $k - 1$ colorants fixed, the remaining colorant ψ_i has only a domain that covers $k - 1$ cells (see Figure 3). The corresponding cell indices are

$$\begin{aligned} I^{i,0} &= (*_0, \dots, *_i, 0, *_i, \dots, *_m) \\ &\vdots \\ I^{i,k-2} &= (*_0, \dots, *_i, k-2, *_i, \dots, *_m) \end{aligned}$$

and the corresponding cell matrices are

$$\begin{bmatrix} [A_i^{i,0}, B_i^{i,0}] \\ \vdots \\ [A_i^{i,k-2}, B_i^{i,k-2}] \end{bmatrix}$$

Since all colorants except ψ_i are fixed we need to calculate the vector $v_i(\psi)$ (see equation (11)) only once. The CYNSEN model in $1/n$ -space in each of the considered cells is

$$\begin{aligned} R(\psi)^{1/n} &= A_i^{i,j} \cdot \vec{v}_i(\psi) \cdot \psi_i + B_i^{i,j} \cdot \vec{v}_i(\psi) \\ &= \vec{A}_i^{i,j}(\psi) \cdot \psi_i + \vec{B}_i^{i,j}(\psi) \end{aligned} \quad (14)$$

where $I^{i,j}$ is the cell that contains ψ .

Using this nomenclature it is sufficient to replace step 3 of the LRI algorithm by the following procedure, where $I^{i,j}$ is the multi-index of the cell containing the actual colorants ψ

1. FOR ($l = 0; l < k - 1; l = l + 1$) {
2. $\psi_i = D \left[\frac{\vec{A}_i^{i,j}(\psi)^T (\vec{B}_i^{i,j}(\psi) - r^{1/n})}{\vec{A}_i^{i,j}(\psi)^T \vec{A}_i^{i,j}(\psi)} \right]$;
3. IF $\psi_i = 0$:
4. IF $j > 0$: $j = j - 1$;
5. ELSE BREAK;
6. ELSE
7. IF $\psi_i = 1$:
8. IF $j < k - 2$: $j = j + 1$;
9. ELSE BREAK;
10. ELSE BREAK;
11. }

By using the matrix scheme AB for each colorant the above procedure accesses matrices in the same columns. The transition from one cell to its neighbor is simply performed through seeking to the corresponding rows. The whole iteration is performed with normalized colorants. There is no need to calculate the actual colorants from the normalized colorants during the iteration. After the sequence converges the resulting normalized control values are then converted to the real effective control values.

We call this algorithm *Cellular Linear Regression Iteration* (CLRI) method.

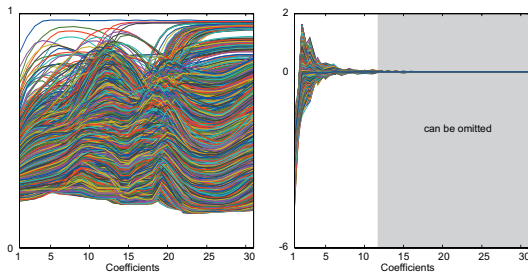


Figure 4. Left: Reflectance spectra of cell primaries in $1/n$ space for $n = 3$. Right: The same reflectance spectra transformed into the subspace by multiplying with U^T .

Acceleration of the Algorithm by small Modifications of the CLRI Method

In the introduction we emphasized the need of spectral gamut mapping, because the spectral gamut of today's printers are limited and not all natural reflectance spectra can be reproduced in an error less way. The fact of a limited dimensionality of the spectral printer gamut can be used as an advantage to save computational effort.

The idea of acceleration is to perform the iteration within a low-dimensional space without changing the convergence behavior. A look closer to the spectral gamut of the printer by examining the set of all spectra that can be reproduced by the CYNSEN model (i.e. $R([0,1]^m)$), shows that all reproducible spectra are lying within a subspace effectively spanned by the cell primaries. This subspace is much lower in dimension than the whole spectral space and could be a good candidate of performing the iteration. But how can we guaranty that the convergence behavior is not affected by the choice of the space? To analyse this we need to investigate the space transformation and the objective function in eq. (4). The objective function is invariant under isometric (i.e. length preserving) transformation. Such isometric transformation is a multiplication with any real valued, unitary matrix. If X is a $N \times N$ dimensional real valued, unitary matrix ($X^T X = X X^T = I$) than the following equation applies

$$\|R(\psi)^{1/n} - r^{1/n}\|_2 = \|X \cdot (R(\psi)^{1/n} - r^{1/n})\|_2$$

To find an appropriate orthonormal transformation for the plain YNSN method, Urban et. al [17] proposed to use the orthogonal matrix resulting from the singular value decomposition (SVD) of the matrix composed of the Neugebauer primaries in $1/n$ -space. This idea can easily be expanded to the CYNSEN model by using all cell primaries in $1/n$ -space. If $R^{1/n} = (R_1^{1/n}, \dots, R_{k^m}^{1/n})$ is the $N \times k^m$ matrix of cell primaries in $1/n$ -space we can decompose the matrix using SVD as follows

$$R^{1/n} = U \cdot S \cdot V^T \quad (15)$$

U is a real valued, $N \times N$ -dimensional, unitary matrix and contains the characteristic spectra of the cell primaries in $1/n$ -space and S contains the singular values $s_i, i = 1, \dots, \min\{N, 2^m\}$, as diagonal elements ordered by their size, i.e. $i < j \Rightarrow s_i \geq s_j$. Only $q \ll N$ singular values are in general significantly larger than zero. In our experiments with two $m = 6$ colorant printers and a CYNSEN model with $k = 4$ gridpoints q was approximately 12. The matrix U can be decomposed into the first q columns that correspond to the first q singular values and the remaining columns, i.e. $U = [U_q, U_{N-q}]$. By multiplying the cell primaries in $1/n$ space by U^T only q components are significantly larger than zero (see Figure 4). Due to this coordinate transform we are able to omit the remaining dimensions and reduce the computational effort significantly. To show that this not affect the convergence

behavior we appraise the objective function as follows:

$$\|R(\psi)^{1/n} - r^{1/n}\|_2 \quad (16)$$

$$= \|U^T \cdot (R(\psi)^{1/n} - r^{1/n})\|_2 \quad (17)$$

$$= \left\| \begin{matrix} U_q^T \cdot R(\psi)^{1/n} - U_q^T \cdot r^{1/n} \\ \underbrace{U_{N-q}^T \cdot R(\psi)^{1/n} - U_{N-q}^T \cdot r^{1/n}}_{\approx 0} \end{matrix} \right\|_2 \quad (18)$$

$$\approx \left\| \begin{matrix} U_q^T \cdot R(\psi)^{1/n} - U_q^T \cdot r^{1/n} \\ U_{N-q}^T \cdot r^{1/n} \end{matrix} \right\|_2 \quad (19)$$

In eq. (19) the second addend (i.e. $\|U_{N-q}^T \cdot r^{1/n}\|_2$) is independent of any colorant value. Since we are interested in colorant values that minimize the objective function we can omit this term and change our objective function (see eq. (4)) into

$$\|U_q^T \cdot R(\psi)^{1/n} - U_q^T \cdot r^{1/n}\|_2 \quad (20)$$

The new problem can be solved by the CLRI method as well. The main advantage is, that we can multiply U_q^T with each matrix AB^l (see eq. (12)) in advance. The only modifications of the method are the multiplication of each reflectance spectrum $r^{1/n}$ with U_q^T and the new matrix scheme

$$AB_q = \begin{bmatrix} U_q^T \cdot AB^{(0,\dots,0)} \\ U_q^T \cdot AB^{(0,\dots,1)} \\ \vdots \\ U_q^T \cdot AB^{(0,\dots,k-2)} \\ U_q^T \cdot AB^{(0,\dots,1,0)} \\ \vdots \\ U_q^T \cdot AB^{(k-2,\dots,k-2)} \end{bmatrix} \quad (21)$$

The main computational effort of the CLRI method is the two matrix-vector multiplication for the linear regressions. By using the above matrix scheme instead of the matrix scheme in eq. (13) the number of rows of each matrix reduces to q instead of N . Each matrix-vector multiplication has than only $q \times 2^{m-1}$ multiplication-operations instead of $N \times 2^{m-1}$. For an effective dimension of $q = 12$ and a usual sampling rate of $N = 31$ we can save more than 60% of the multiplications.

We called this method the *Subspace Cellular Linear Regression Iteration* (SCLRI) method.

Results

To test the SCLRI method we utilize the cell primaries of a $k = 3$ and $k = 4$ gridpoint CYNSEN model of a HP Designjet Z3100 Photo printer. Only the CMYKRG subset of the available inks of this printer was used. To ensure that the test spectra are within the spectral gamut of the printer we generated 1 million control value combinations and processed them through the forward model. The resulting spectra were used for the separation. The control value combinations used in the experiment were

$$\{0, 3, 7, 14, 24, 41, 65, 104, 163, 255\}^6 \quad (22)$$

Results for optimal q value

	3 gridpoints	4 gridpoints
A, mean(ΔE_{00})	0.45	0.41
A, max(ΔE_{00})	15.78	19.01
D50, mean(ΔE_{00})	0.45	0.41
D50, max(ΔE_{00})	15.87	19.80
F11, mean(ΔE_{00})	0.52	0.47
F11, max(ΔE_{00})	13.55	21.7
mean(RMS)	0.003	0.003
std(RMS)	0.005	0.006
max(RMS)	0.091	0.091
time [s]	126	312

To adjust the cell primaries to the model we used the method proposed by Chen et al. [20]. The Yule-Nielsen factor was $n = 10$. To test the accuracy of the SCLRI method for different q values, we performed the separation using $q = 1, \dots, 31$. For $q = 31$ the SCLRI method is similar to the CLRI method, since the sampling rate is $N = q = 31$. The starting point for each iteration is paper white, i.e. $(C, M, Y, K, R, G) = (0, 0, 0, 0, 0, 0)$. The calculations has been performed using C++ on an AMD Athlon X2 4200+ system. Figure 5 shows the mean spectral RMS results and the calculation time. Table 1 shows colorimetric and spectral RMS results for the optimal q value, i.e. $q = 10$ for 3 gridpoint CYNSEN model and $q = 12$ for the 4 gridpoint CYNSEN model.

The large maximal colorimetric errors result from separations of very dark colors where colorimetric errors does not correlate with spectral RMS errors. Dark colors with a very small spectral RMS difference can have a large colorimetric difference. Since we are minimizing spectral differences large colorimetric errors can be the consequence. The algorithm can be

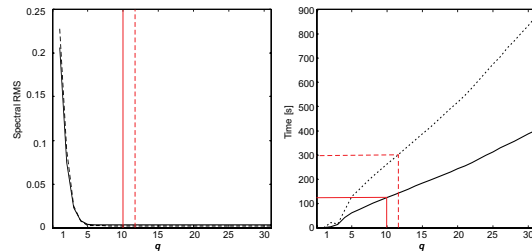


Figure 5. Left: Mean spectral RMS error for different q -values. Right: Calculation time to separate 1 million spectra. Solid lines used for 3 gridpoint CYNSEN, dashed lines for 4 gridpoint CYNSEN. Red lines indicate the smallest q value of the SCLRI method with equal results to the CLRI method.

further significantly accelerated by using spatial information of multispectral images. Since neighboring pixels of natural images tend to be highly correlated the starting point of the iteration can be chosen as the resulting separation of the previous calculated neighboring pixel. This simple procedure avoid many transitions of the iteration.

Conclusion

In this paper we present an algorithmic framework for spectral separation of multispectral images. The proposed iterative

method inverts the widely used cellular Yule-Nielsen spectral Neugebauer model using mainly simple matrix-vector multiplications in each iteration step. The transition of the iteration from cell to cell is performed by choosing the correct matrix from a pre-calculated matrix scheme. Small modifications of the algorithm significantly reduce the computational effort by performing the iteration within the subspace effectively spanned by the cell primaries in $1/n$ -space. Using today's available standard hardware allows the separation of high resolution multispectral images in reasonable time.

Acknowledgements

The authors thank HP for providing the printer and supplies, Onyx for providing the RIP and the Deutsche Forschungsgemeinschaft (German Research Foundation) for the sponsorship of this project.

References

- [1] ICC. *File Format for Color Profiles*. <http://www.color.org>, 4.0.0 edition, 2002.
- [2] M.R. Rosen and M.W. Derhak. Spectral Gamuts and Spectral Gamut Mapping. In *Spectral Imaging: Eighth International Symposium on Multispectral Color Science*, San Jose, CA, 2006. SPIE.
- [3] D.-Y. Tzeng and R. S. Berns. Spectral-Based Six-Color Separation Minimizing Metamerism. In *IS&T/SID*, pages 342–347, Scottsdale Ariz., 2000.
- [4] Y. Chen, R. S. Berns, L. A. Taplin, and F. H. Imai. A Multi-Ink Color-Separation Algorithm Maximizing Color Constancy. In *IS&T/SID*, pages 277–281, Scottsdale Ariz., 2003.
- [5] D. R. Wyble and R. S. Berns. A Critical Review of Spectral Models Applied to Binary Color Printing. *Color Research and Application*, 25:4–19, 2000.
- [6] H. E. J. Neugebauer. Die theoretischen Grundlagen des Mehrfarbenbuchdrucks. *Zeitschrift für wissenschaftliche Photographie, Photophysik und Photochemie [translation in 7]*, 36:73–89, 1937.
- [7] H. E. J. Neugebauer. The Theoretical Basis of Multicolor Letterpress Printing (Translated D. Wyble and A. Kraushaar). *Color Research and Application*, 30:322–331, 2005.
- [8] J. A. C. Yule and W. J. Nielsen. The penetration of light into paper and its effect on halftone reproduction. In *Tech. Assn. Graphic Arts*, volume 4, pages 65–76, 1951.
- [9] J. A. C. Yule and R. S. Colt. Colorimetric Investigations in Multicolor Printing. In *TAGA Proceedings*, pages 77–82, 1951.
- [10] J.A.S. Viggiano. The Color of Halftone Tints. In *TAGA Proceedings*, pages 647–661, 1985.
- [11] J.A.S. Viggiano. Modeling the Color of Multi-color Halftones. In *TAGA Proceedings*, pages 44–62, 1990.
- [12] K. J. Heuberger, Z. M. Jing, and S. Persiev. Color transformations from lookup tables. In *TAGA Proceedings*, pages 863–881, 1992.
- [13] S. Zuffi and R. Schettini. Spectral-Based Printer Characterization. In *CGIV*, pages 598–602, Poitiers, France, 2002. IS&T.
- [14] L. A. Taplin. Spectral Modeling of a Six-Color Inkjet Printer, MSc. thesis. RIT, NY, 2001. MSc. thesis. RIT, NY, 2001.
- [15] D.-Y. Tzeng. *Spectral-Based Color Separation Algorithm Developed for Multiple-Ink Color Reproduction*. PhD thesis.
- [16] P. Urban and R.-R. Grigat. Spectral-Based Color Separation using Linear Regression Iteration. *Color Research and Application*, 31:229–238, 2006.
- [17] P. Urban, M. R. Rosen, and S. Berns R. Accelerating spectral-based color separation within the neugebauer subspace. *Journal of Electronic Imaging (in press)*, 2007.
- [18] P. Urban and M. R. Rosen. Inverting the Cellular Yule-Nielsen modified Spectral Neugebauer Model. In *Ninth International Symposium on Multispectral Color Science and Application*, pages 29–35, Taipei, Taiwan, 2007.
- [19] A. U. Agar and J. P. Allebach. An iterative cellular ynsn method for color printer characterization. In *IS&T/SID*, pages 197–200, Scottsdale Ariz., 1998.
- [20] Y. Chen, R. S. Berns, and L. A. Taplin. Six color printer characterization using an optimized cellular Yule-Nielsen spectral Neugebauer model. *Journal of Imaging Science and Technology*, 48:519–528, 2004.

Author Biography

Philipp Urban received his M.S. degree in Mathematics from the University of Hamburg in 1999 and his Dr. degree in the field of color science from the Hamburg University of Technology in 2005. From 1999 until 2006 he was part of the research group "Vision Systems" at the Hamburg University of Technology and worked for Ratio Entwicklungen GmbH (ICC-member) where he developed color managing systems. Since 2006 he is a visiting scientist at the Munsell Color Science Laboratory at the Rochester Institute of Technology. His research interests are color science and multispectral imaging.